ISSN 1990-7931, Russian Journal of Physical Chemistry B, 2022, Vol. 16, No. 6, pp. 1057–1066. © Pleiades Publishing, Ltd., 2022.
Russian Text © The Author(s), 2022, published in Khimicheskaya Fizika, 2022, Vol. 41, No. 12, pp. 26–35.

KINETICS AND MECHANISM OF CHEMICAL REACTIONS, CATALYSIS

Dynamics of Direct Three-Body Recombination of Cesium and Fluoride Ions As Well As of Cesium and Iodide Ions in the Presence of a Krypton Atom

V. M. Azriel'[a], V. M. Akimov[a], E. V. Ermolova[a], D. B. Kabanov[a], L. I. Kolesnikova[a], L. Yu. Rusin[a, *], and M. B. Sevryuk[a]

[a] *Tal'rose Institute for Energy Problems of Chemical Physics, Semënov Federal Research Center for Chemical Physics, Russian Academy of Sciences, Moscow, 119334 Russia*

**e-mail: rusin@chph.ras.ru*

Received February 28, 2022; revised March 16, 2022; accepted March 21, 2022

Abstract—Within the framework of the quasiclassical trajectory method and using semiempirical diabatic potential energy surfaces, we have studied statistical dynamics of two reactions of direct three-body recombination, $Cs^+ + X^- + Kr \rightarrow CsX + Kr$ ($X^- = F^-$, I^-), with non-central encounters of the ions. The collision energies range between 1 and 10 eV, while the so-called delay parameter, which characterizes the delay in the arrival of the krypton atom with respect to the time instant when the distance between the recombining cesium and halide ions attains its minimum, is equal to 0 or 0.2. We have found the excitation functions of recombination, the opacity functions, the vibrational energy distributions of the CsX product (which turn out to be strongly non-equilibrium), and the CsX rotational energy distributions (which are almost equilibrium). A comparison with the calculation results for the reactions $Cs^+ + X^- + Ar$ and $Cs^+ + X^- + Xe$ published earlier shows that, on the whole, for both the recombining ion pairs $Cs^+ + F^-$ and $Cs^+ + I^-$, the heavier the third body, the more effective it is as an acceptor of excess energy of the ion pair.

Keywords: statistical dynamics of elementary processes, direct three-body recombination of ions, trajectory simulation, cesium cation, fluoride and iodide anions, krypton

DOI: 10.1134/S1990793122060148

1. INTRODUCTION

Recombination reactions of atoms, ions, or radicals and reverse reactions of collision induced dissociation (CID) constitute two classes of processes that are key for describing very many high-temperature gas and plasma media, of both natural and artificial origin. For instance, of the 196 reactions identified as important in combustion chemistry in the work [1], about half are recombination or CID reactions [2, 3]. Recent studies of the effects of recombination processes on the combustion rate and on the flame structure are exemplified by the papers [4, 5]. The recombination and CID reactions are largely responsible for the concentration of ions in plasma media, especially in the plasma of electronegative gases (whose particles are able to capture free electrons and turn into stable negative ions) [6, 7], whereas the processes of three-body recombination of active centers lead to a quadratic termination of chain transformations [8–10] (recent studies in this area are discussed in, e.g., the review [11]). Recombination of ions in low-temperature plasma (LTP) plays a significant role in solving various practically important tasks, for instance, in technologies for obtaining new materials or in treating the surfaces of solids in order to impart the necessary properties to them [12]. Reactions of atom-atom and ion-ion recombination in the atmosphere of Earth and of other planets were considered in, e.g., the recent papers [13–15]. Three-body ion-ion recombination is one of the most important processes in the kinetics of the active media of rare gas monohalide excimer lasers [16–18].

Since the mid 2000s, in the Laboratory for Dynamics of Elementary Processes of the Tal'rose Institute for Energy Problems of Chemical Physics of the Russian Academy of Sciences (since 2019, one of the subdivisions of the Semënov Federal Research Center for Chemical Physics of the Russian Academy of Sciences), there have been carried out systematic studies of the dynamics of direct three-body recombination of singly charged heavy ions

$$Cs^+ + X^- + R \rightarrow CsX + R, \qquad (1)$$

where X^- is the halide ion F^-, Br^-, or I^- and R is the rare gas atom Ar, Kr, Xe or mercury atom Hg which takes away excess energy of the recombining ion pair $Cs^+ + X^-$ [19–34]. There are currently no methods for experimentally determining the dynamical character-

istics of direct three-body recombination, mainly because it is extremely difficult to achieve experimentally the intersection of three sufficiently intensive beams or of two beams and a dense gas target. In addition, it is not clear how to distinguish the products of three-body collisions from those of pairwise scattering of the particles, in particular (when it comes to recombination (1)), from the products of bimolecular recombination

$$RCs^+ + X^- \rightarrow CsX + R \quad (2)$$

which has also been explored in the Laboratory for Dynamics of Elementary Processes [32, 35]. Finally, what is also a very difficult task is to identify excited pair complexes and excited products of three-body recombination, as well as to take into account a significant number of side reactions occurring in discharges, especially in electronegative gases [6]. Therefore, the only way to examine the dynamics of direct three-body recombination reactions is quantum mechanical, semiclassical, or quasiclassical simulation (as well as, in some cases, using hard sphere models).

In the works [19–28, 30–34], the reactions (1) and (2) were studied within the framework of the quasiclassical trajectory method on semiempirical diabatic potential energy surfaces (PESs). The adequacy of these PESs is confirmed by the fact that they provide, again within quasiclassical trajectory simulation, a quantitative reproduction of many dynamical characteristics (obtained in experiments with crossed molecular beams) of the reverse CID reactions

$$CsX + R \rightarrow Cs^+ + X^- + R,\ RCs^+ + X^-. \quad (3)$$

It follows from the principle of microscopic reversibility that the recombination reactions (1), (2) and the CID reactions (3) are governed by the same PESs. Note that the CID channel $CsX + R \rightarrow RX^- + Cs^+$ was observed in experiments with crossed molecular beams for the system CsI + Xe only [36, 37]. In the papers [29, 35], hard sphere models of the reactions (1) and (2) were proposed. In the works [19–32, 35], only the bromide ion Br^- was considered in the role of the halide ion X^-. In the recent papers [33, 34], we explored the dynamics of four reactions (1) with $X^- = F^-$, I^- and R = Ar, Xe.

While simulating an elementary process by the quasiclassical trajectory method, each trajectory is determined by certain values of the kinematic parameters which constitute the collection of initial conditions. As a rule, some of these parameters (e.g., the collision energies) are set to be fixed within the given calculation, while the other parameters are chosen randomly with averaging various quantities computed at the end of the trajectory integration. Such a Monte Carlo approach enables one to study *statistical* dynamics of the process and to find its main dynamical characteristics (the results of averaging) which can be compared with experimental data (provided that such data are available) and to assess the adequacy of the PES employed. On the other hand, while one examines *detailed* dynamics of the process, averaging over the trajectories is absent (or minimized) and a step-by-step analysis of individual trajectories is carried out. The most effective tool for studying the dynamics of the system within a single trajectory is visualization of the trajectory. The results of visualization of trajectories describing direct three-body recombination (1) are presented in the works [19, 21–24, 26–28, 34]. Visualization of trajectories describing the CID reactions (3) was carried out in, e.g., the papers [38, 39] (in the work [39], both the CID channels were considered).

In the paper [33], we thoroughly explored statistical dynamics of direct three-body recombination (1) with $X^- = F^-$, I^- and R = Ar, Xe in the collision energy range from 1 to 10 eV (values typical for LTP [6, 7]). In the present paper, which is an immediate continuation of the work [33], we study statistical dynamics of direct three-body recombination (1) with $X^- = F^-$, I^- and R = Kr, also in the collision energy range from 1 to 10 eV. As in [33], we determine the recombination excitation functions, the opacity functions, and the distributions of the vibrational and rotational energies of the CsF and CsI molecules. The results obtained confirm the general patterns noted in [33] of the dependences of the dynamical characteristics of recombination (1) on the halide ion and the third body.

The paper is organized as follows. In Section 2, we briefly characterize the PESs of the systems $Cs^+ + F^- + Kr$ and $Cs^+ + I^- + Kr$ that we employ and the features of the choice of the kinematic parameters of the trajectories. The calculation results are presented in Sections 3 and 4. The remarks of Section 5 conclude the work.

2. POTENTIAL ENERGY SURFACES AND KINEMATIC PARAMETERS

As in all our previous works devoted to trajectory simulation of the recombination reactions (1), (2) and the CID reactions (3) (see e.g. [19–28, 30–34, 39]), in the present paper we used semiempirical diabatic PESs which were the sum of three pairwise potentials and a cross term corresponding to the polarization interaction in the system of the R atom and the Cs^+–X^- dipole. In all these PESs, the ionic interaction potential Cs^+–X^- was given by the standard truncated Rittner model [40, 41]:

$$U(r) = Ae^{-r/\rho} - 1/r - \left(\alpha_{Cs^+} + \alpha_{X^-}\right)/\left(2r^4\right) - C/r^6 \quad (4)$$

(in the atomic units), whereas the interaction potentials Cs^+–R and X^-–R for R = Ar, Kr, Xe were given by the model [38]:

$$U(r) = Ae^{-r/\rho} - \alpha_R/\left(2r^4\right) - C/r^6. \quad (5)$$

In the expressions (4) and (5), r is the internuclear distance, A and ρ are the repulsive Born–Mayer parameters, C is the dispersion constant of the van der Waals interaction in the London approximation, and α_{Cs^+}, α_{X^-}, α_R are the polarizabilities of the particles. The expression for the cross term only involves the pairwise internuclear distances and the polarizabilities of the particles. The complete expression for the PESs employed in the present paper is given in, e.g., the works [20–26, 28, 30, 33].

We used the same values of the polarizabilities α_{Cs^+}, α_{F^-}, α_{I^-} and the same values of the parameters A, ρ, C for the interaction potentials $Cs^+–F^-$ and $Cs^+–I^-$ as in the works [33, 34] (these values are presented in the paper [33]). The polarizability α_{Kr} of the krypton atom was set to be equal to 16.8 a.u. [36, 42–44]. The values of the parameters A, ρ, C for the interaction potentials $Cs^+–Kr$, $F^-–Kr$, and $I^-–Kr$ that we utilized are collected in Table 1. These values were obtained on the basis of various sources [36, 42–49]. Some parameters are explicitly given in these works while the other ones were computed to ensure the reproduction of the spectroscopic data, i.e., of the location R_m and depth D of the potential well. Note that a detailed annotated bibliography of the works (up to 2016) on the interaction potentials in all the two-particle systems $M^+–X^-$, $M^+–R$, $X^-–R$, and R–Hg (M^+ being an alkali ion, X^- a halide ion, and R a rare gas atom) is presented in the report [50].

Direct three-body recombination (1) with non-central encounters of the ions was considered in the works [22, 26, 27, 29, 30, 33, 34]. Of these works, the papers [22, 26, 30, 33] were devoted to studying statistical dynamics of recombination (1) within the framework of the quasiclassical trajectory method. The procedures for choosing the initial conditions of the trajectories and the organization of calculations in those papers did not differ much from each other. In the present work, we employed exactly the same procedures for choosing the initial conditions, integrating the trajectories, and computing the dynamical characteristics of recombination as in the paper [33]. Here we only note that for simulating direct three-body recombination (1) with non-central encounters of the ions, eight kinematic parameters are required to set the initial conditions of the trajectories (see a detailed discussion in [34]):

the ion encounter energy (the energy of approach of the ions) E_i, i.e., the initial kinetic energy of the relative motion of the ions,

the third body energy E_R, i.e., the initial kinetic energy of the relative motion of the R atom and the ion pair $Cs^+–X^-$,

the impact parameter b_i of the ion encounter,

Table 1. The parameters of the interaction potentials $Cs^+–Kr$, $F^-–Kr$, and $I^-–Kr$ (in the atomic units)

Pair of the particles	A	ρ	C	References
$Cs^+–Kr$	796	0.5281	247.1	[36, 42, 44–48]
$F^-–Kr$	77.1	0.55	69.6	[43–45, 49]
$I^-–Kr$	332.5	0.633	322.4	[43–45]

the impact parameter b_R of the third body R with respect to the center of mass of the ion pair,

three orientation angles Θ, Φ, γ (which specify, together with E_i and b_i, the initial positions and velocities of the ions),

the delay parameter T_{del} [26, 30, 33, 34]. The dimensionless quantity $T_{del} \geq -1$ measures the delay (for $T_{del} > 0$) or the outstripping (for $T_{del} < 0$) in the arrival of the third body in relation to approach of the ions (to be more precise, in relation to the time instant when the distance between the ions attains its minimum). In most calculations, the delay parameter is assumed to be zero. We always set the initial internuclear distance d_i between the ions to be equal to 250 a.u.

The presence of two collision energies E_i and E_R and of two impact parameters b_i and b_R is a characteristic feature of simulating direct three-body recombination by the quasiclassical trajectory method. The equality $b_i = 0$ corresponds to the case of central (or head-on) encounters of the recombining ions. The initial configurations of the particles for direct three-body recombination (1) with non-central encounters of the ions are shown schematically in the papers [22, 26]. While analyzing statistical dynamics of direct three-body recombination (1), one fixes certain values of the delay parameter T_{del} and of the collision energies E_i and E_R, after which one integrates sufficiently many (several hundreds of thousands) trajectories with the parameters b_i, b_R, Θ, Φ, γ to be varied.

In all the calculations in the work [33] and in the present paper, the maximal values of the impact parameters b_i and b_R *chosen* as initial conditions were set to be equal to $b_{i,max} = 40$ a.u. and $b_{R,max} = 100$ a.u., respectively, whereas the delay parameter T_{del} was assumed to be equal to 0 or 0.2. Several test calculations have shown that for larger impact parameters, recombination in the systems under study never occurs for these values of T_{del} and for the collision energies E_i, E_R between 1 and 10 eV. The quantities $(b_i / b_{i,max})^2$ and $(b_R / b_{R,max})^2$ are chosen uniformly between 0 and 1. As in the work [33], the maximal values of the impact parameters b_i and b_R for which we *actually* observed recombination (in the given system

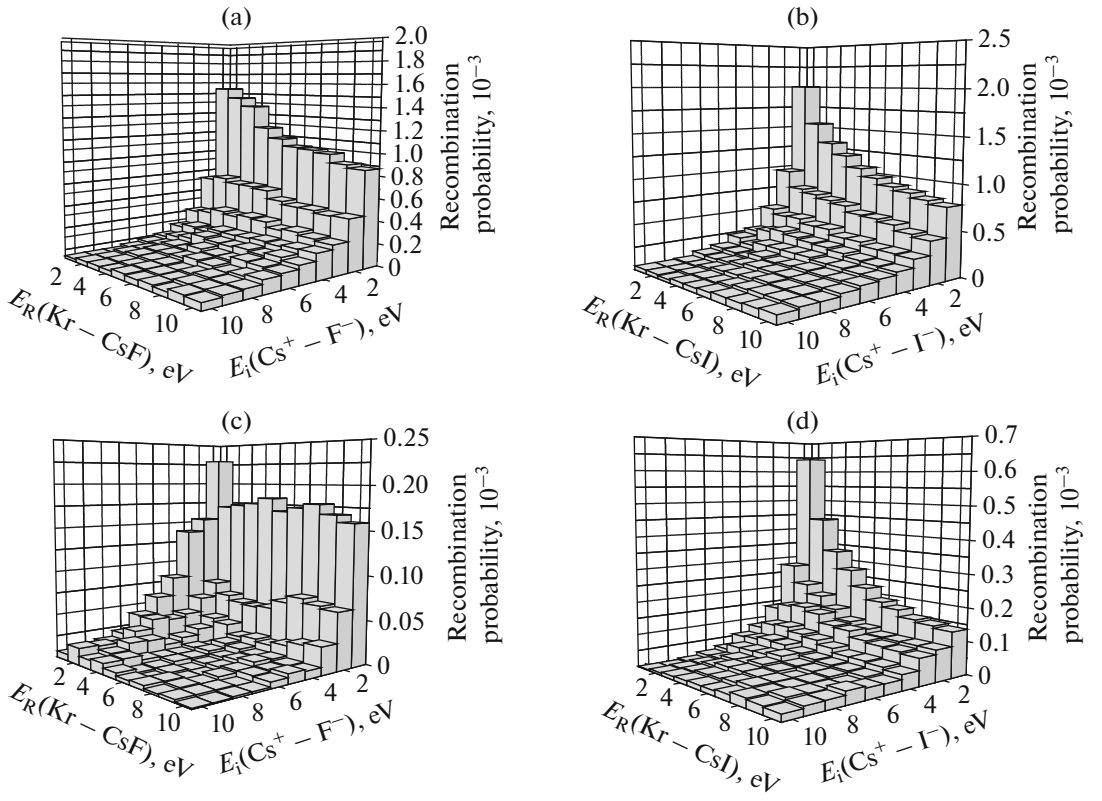

Fig. 1. (a) The excitation function of recombination $Cs^+ + F^- + Kr$ at $T_{del} = 0$. (b) The excitation function of recombination $Cs^+ + I^- + Kr$ at $T_{del} = 0$. (c) The excitation function of recombination $Cs^+ + F^- + Kr$ at $T_{del} = 0.2$. (d) The excitation function of recombination $Cs^+ + I^- + Kr$ at $T_{del} = 0.2$. The recombination probabilities are presented in units of 10^{-3}, i.e., the probability values are 10^3 times smaller than the numbers indicated on the applicate axes.

at the given fixed parameters T_{del}, E_i, E_R) are denoted in Section 4 below by $b_{i,lim}$ and $b_{R,lim}$, respectively. These values can be significantly smaller than the values $b_{i,max}$ and $b_{R,max}$ (since the latter values were set "with a margin").

3. EXCITATION FUNCTIONS

In the present paper, as in the work [33], we will call the dependence $P(E_i, E_R)$ of the recombination probability on the collision energies E_i and E_R at a fixed value of the delay parameter T_{del} the excitation function, although the excitation function for bimolecular reactions is defined as the dependence of the reaction cross section (rather than of the reaction probability) on the collision energy. Figures 1a, 1b shows the excitation functions $P(E_i, E_R)$ of the direct three-body recombination reactions

$$\begin{aligned} Cs^+ + F^- + Kr \rightarrow CsF + Kr, \\ Cs^+ + I^- + Kr \rightarrow CsI + Kr \end{aligned} \quad (6)$$

at $T_{del} = 0$. As in the work [33], for both the reactions, each of the collision energies was varied from 1 to 10 eV with a step of 1 eV, so the excitation functions are portrayed as two-dimensional diagrams consisting of 100 elements.

In Table 2 for the six reactions (1) with $X^- = F^-$, I^- and R = Ar, Kr, Xe, we present the recombination probabilities at $T_{del} = 0$ averaged in five different ways:

over all the 100 pairs (E_i, E_R),

over the 50 pairs (E_i, E_R) with $1 \le E_i \le 5$ eV and over the 50 pairs (E_i, E_R) with $6 \le E_i \le 10$ eV,

over the 50 pairs (E_i, E_R) with $1 \le E_R \le 5$ eV and over the 50 pairs (E_i, E_R) with $6 \le E_R \le 10$ eV.

Besides that, in Table 2 for all the six reactions, we point out the coefficients of correlation between the recombination probability $P(E_i, E_R)$ and the third body energy E_R at low fixed ion encounter energies $E_i = 1$, 2, and 3 eV. These correlation coefficients show how close is the dependence of the recombination probability on E_R to its "linear component" [51, 52]. All the data of Table 2 related to the reactions (1)

Table 2. The recombination probabilities in the systems (1) with $X^- = F^-$, I^- and R = Ar, Kr, Xe at $T_{del} = 0$ averaged over the collision energies and presented in units of 10^{-7} (the actual values of the probabilities are 10^7 times smaller than the numbers given in the table)

System	$Cs^+ + F^- + R$		$Cs^+ + I^- + R$	
Averaging over all the 100 pairs (E_i, E_R)				
R = Ar	2482		1832	
R = Kr	2746		3181	
R = Xe	3054		3565	
Averaging over $1 \le E_i \le 5$ eV, $1 \le E_R \le 10$ eV and over $6 \le E_i \le 10$ eV, $1 \le E_R \le 10$ eV				
E_i, eV	1–5	6–10	1–5	6–10
R = Ar	4034	930	3411	253
R = Kr	4714	778	5350	1013
R = Xe	5444	665	5910	1221
Averaging over $1 \le E_i \le 10$ eV, $1 \le E_R \le 5$ eV and over $1 \le E_i \le 10$ eV, $6 \le E_R \le 10$ eV				
E_R, eV	1–5	6–10	1–5	6–10
R = Ar	2912	2051	1808	1856
R = Kr	2910	2581	3583	2779
R = Xe	3056	3052	4336	2795
The coefficients of correlation between the recombination probability and the energy E_R at E_i = 1, 2, and 3 eV				
R = Ar	–0.87; –0.82; –0.86		–0.95; –0.47; 0.79	
R = Kr	–0.96; –0.94; –0.45		–0.92; –0.96; –0.98	
R = Xe	–0.92; –0.14; 0.76		–0.92; –0.95; –0.94	

with $X^- = F^-$, I^- and R = Ar, Xe are given in the work [33], and we reproduce them in the present paper for the reader's convenience. Note the misprint in [33]: for the reaction $Cs^+ + I^- + Xe$, the coefficient of correlation between $P(1\text{ eV}, E_R)$ and E_R is equal to –0.92 rather than to –0.95 as is pointed out in Table 2 in [33].

Based on Figs. 1a, 1b of the present paper, on Figs. 3 and 4 in the work [33] (those two figures pertain to the reactions (1) with $X^- = F^-$, I^- and R = Ar, Xe), and on the data of Table 2, one can draw the following conclusions about the behavior of the excitation functions $P(E_i, E_R)$ of the six reactions in question of direct three-body recombination (1) with non-central encounters of the ions at $T_{del} = 0$.

First, the heavier the neutral atom R, the more effective it is, on the whole, as an acceptor of excess energy of the recombining ion pair $Cs^+ + X^-$ with $X^- = F^-$, I^-. The same observation takes place for the reactions (1) with $X^- = Br^-$ [30]. For both the halide ions F^- and I^-, the recombination probability averaged over all the 100 pairs (E_i, E_R) monotonously increases as one passes from R = Ar to R = Kr and then to R = Xe (see Table 2). The same holds for the recombination probability averaged over the 50 pairs (E_i, E_R) with $1 \le E_i \le 5$ eV (for both the halide ions), with $6 \le E_i \le 10$ eV (for $X^- = I^-$), with $1 \le E_R \le 5$ eV (for $X^- = I^-$), and with $6 \le E_R \le 10$ eV (for both the halide ions). It is interesting that, on the contrary, the recombination probability averaged over the 50 pairs (E_i, E_R) with $6 \le E_i \le 10$ eV for $X^- = F^-$ is maximal at R = Ar and is minimal at R = Xe.

The conjecture may arise that the growth of the effectiveness of the third body R in the sequence Ar → Kr → Xe is due not only to the increase in the atom mass but also to the enhancement of the bond energies in the systems Cs^+–R and X^-–R. However, there are several arguments against such a conjecture. The potential well depth D is equal to 0.1201, 0.2506, 0.4442 eV in the interaction potentials F^-–Ar, F^-–Kr, F^-–Xe that we used, respectively, and it is equal to 0.0587, 0.0605, 0.0929 eV in the interaction potentials I^-–Ar, I^-–Kr, I^-–Xe, respectively (see Table 1 and the paper [33]). Thus, in the systems X^-–R, the bond energy does grow monotonously as the mass of the atom R increases. On the other hand, in the interaction potentials Cs^+–Ar, Cs^+–Kr, Cs^+–Xe, the potential well depth D is equal to 0.0735, 0.121, 0.1085 eV, respectively, i.e., the bond energy in the system Cs^+–Kr is greater than that in the system Cs^+–Xe (this is consistent with the data of the works [44, 46, 48]). Besides that, for any of the three atoms R, the potential well depth D in the F^-–R interaction potential is much larger than that in the I^-–R interaction poten-

tial (and the potential well depth D in the interaction potentials $Cs^+–F^-$ and $Cs^+–I^-$ is equal to 5.768 and 4.251 eV, respectively). At the same time, as one passes from the reaction $Cs^+ + F^- + R$ to the reaction $Cs^+ + I^- + R$ at R = Kr and R = Xe, the recombination probability averaged over all the 100 pairs (E_i, E_R) increases, and it decreases at R = Ar only (see Table 2). It is worthwhile to note that such a direction of change in the recombination probability as one passes from the reaction $Cs^+ + F^- + R$ to the reaction $Cs^+ + I^- + R$ persists if one considers the probabilities averaged over each of the four sets of 50 pairs (E_i, E_R) indicated above. The only exception is that for R = Xe, the recombination probability averaged over the 50 pairs (E_i, E_R) with $6 \le E_R \le 10$ eV decreases.

Second, the recombination probability $P(E_i, E_R)$ depends on the ion encounter energy E_i to a much greater extent than on the third body energy E_R, and it almost always decreases as E_i grows (all the few exceptions correspond to the energies $E_i \ge 9$ eV for which the relative statistical uncertainties become too significant). The same observation takes place for the reactions (1) with $X^- = Br^-$ [26, 30]. In the diagram of Fig. 2b in [22] for the reaction $Cs^+ + Br^- + Xe$, an opposite situation is presented, but this contradiction is seeming and is caused by a misprint, namely, the titles "E_{rel}(Xe–CsBr), eV" and "$E_{ini}(Cs^+–Br^-)$, eV" of the diagram axes were swapped. As is seen in Table 2, for all the six systems in question, the recombination probability $P(E_i, E_R)$ averaged over the 50 pairs (E_i, E_R) with $1 \le E_i \le 5$ eV is much larger than the recombination probability averaged over the 50 pairs (E_i, E_R) with $6 \le E_i \le 10$ eV. Moreover, in this setting, for both the halide ions F^- and I^-, as the ion encounter energy E_i grows, the Ar atom exhibits the minimal drop in effectiveness while the Xe atom exhibits the maximal drop. For all the six systems, the difference between the recombination probabilities averaged over the 50 pairs (E_i, E_R) with $1 \le E_R \le 5$ eV and over the 50 pairs (E_i, E_R) with $6 \le E_R \le 10$ eV is incomparably less than that in the case of the separation of the diagram elements along the E_i energy (moreover, for the reaction $Cs^+ + I^- + Ar$, this difference is even negative).

For the reactions (6), consider more minutely the dependence of the recombination probability $P(E_i, E_R)$ on the third body energy E_R at low fixed ion encounter energies $E_i = 1$, 2, and 3 eV where the relative statistical uncertainties are small (see Figs. 1a, 1b). The probability $P(1\text{ eV}, E_R)$ for both the reactions and the probability $P(2\text{ eV}, E_R)$ for the reaction $Cs^+ + I^- + Kr$ monotonously decrease as E_R grows. The same holds for the probability $P(3\text{ eV}, E_R)$ for the reaction $Cs^+ + I^- + Kr$ with the only exception: $P(3\text{ eV}, 2\text{ eV}) < P(3\text{ eV}, 3\text{ eV})$. The probabilities $P(2\text{ eV}, E_R)$ and $P(3\text{ eV}, E_R)$ for the reaction $Cs^+ + F^- + Kr$ are not monotonously decreasing functions of the E_R energy. Moreover, the maximum of $P(2\text{ eV}, E_R)$ for this reaction is attained at $E_R = 2$ eV whereas the maximum of $P(3\text{ eV}, E_R)$ is attained at $E_R = 3$ eV and $E_R = 5$ eV (and the coefficient of correlation between $P(3\text{ eV}, E_R)$ and E_R is less than 0.5 in absolute value, see Table 2).

As one passes from zero delay parameter to $T_{del} = 0.2$, the recombination probabilities are reduced sharply and the entire structure of the excitation functions $P(E_i, E_R)$ changes, this change being different for different reactions (1) with $X^- = F^-$, I^- and R = Ar, Kr, Xe, see Figs. 5 and 6 in the work [33] and Figs. 1c, 1d in the present paper. On the whole, the transformation of the structure of the excitation functions of the reactions (6) turns out to be more or less the same as in the case of the reactions (1) with R = Xe and $X^- = F^-$, I^-, respectively, but not as in the case of the reactions (1) with R = Ar and $X^- = F^-$, I^-. In particular, in the diagram of Fig. 1c (R = Kr, $X^- = F^-$), it is the recombination probabilities at $E_i = 1$ eV that "absolutely dominate", while in the diagram of Fig. 1d (R = Kr, $X^- = I^-$), it is the recombination probability at $E_i = E_R = 1$ eV that "absolutely dominates". We also observed a strong drop in the recombination probabilities as one passes from $T_{del} = 0$ to positive values of T_{del} in the case of the reactions (1) with $X^- = Br^-$ [26, 30].

4. OPACITY FUNCTIONS AND DISTRIBUTIONS OF THE INTERNAL ENERGY OF THE RECOMBINATION PRODUCTS

In Table 3, for four combinations of the collision energies $(E_i, E_R) = (1, 1), (1, 5), (5, 1), (5, 5)$ (in eV), we present the maximal values $b_{R,lim}$ and $b_{i,lim}$ of the impact parameter b_R of the third body and of the impact parameter b_i of the ion encounter for which we observed the reactions of direct three-body recombination (6) at $T_{del} = 0$. Figure 2 displays the opacity functions of the recombination reactions (6), i.e., the dependences of the recombination probability on b_R or on b_i, at $T_{del} = 0$ for these four combinations of the collision energies. In the work [33] at $T_{del} = 0$ for the same four combinations of the collision energies, we presented the opacity functions of the reactions (1) with $X^- = F^-$, I^- and R = Ar, Xe. An analysis of all the figures shows that for each halide ion X^- and for each combination of the collision energies (E_i, E_R), the opacity functions corresponding to all the three atoms R = Ar, Kr, and Xe, are rather similar on the whole,

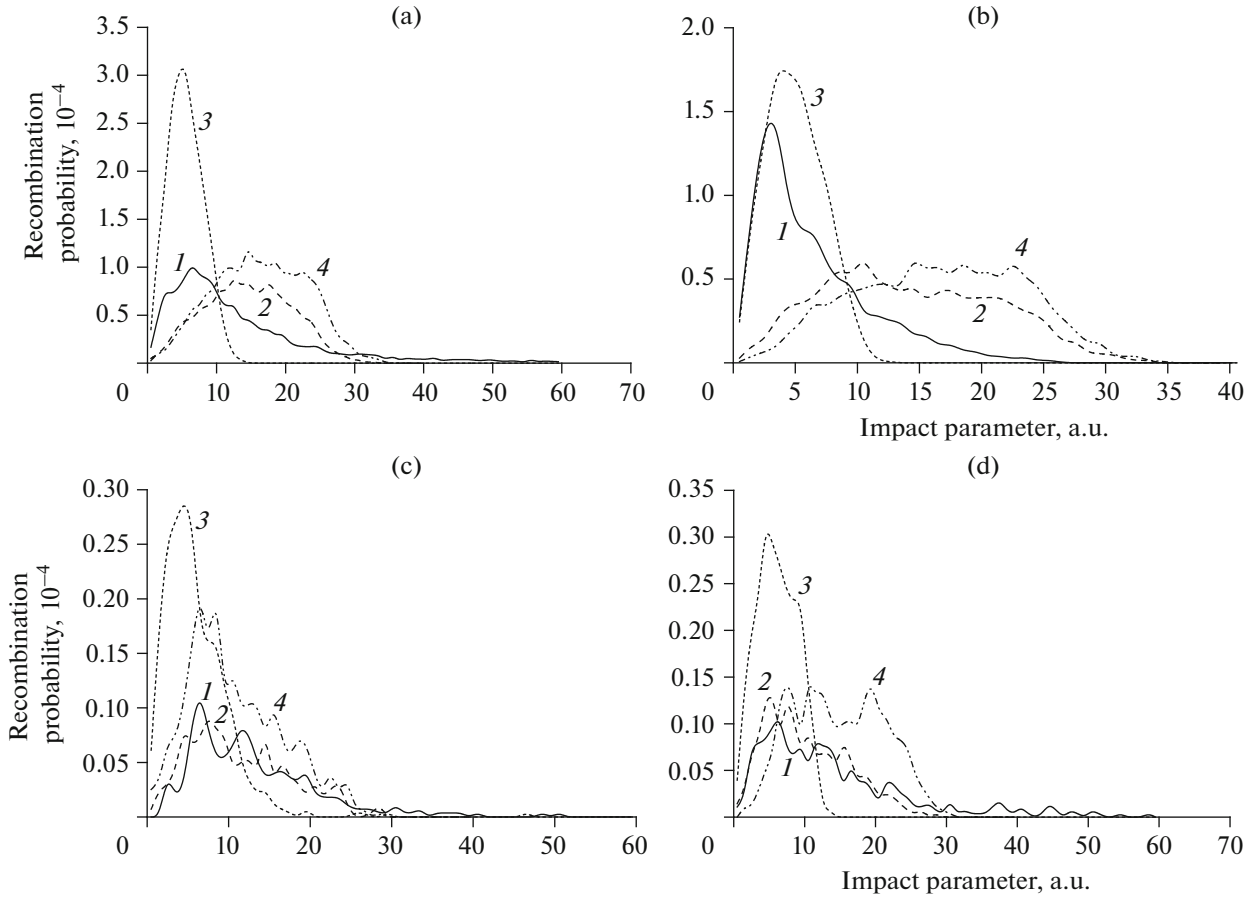

Fig. 2. The b_R (lines *1*) and b_i (lines *2*) opacity functions of the recombination reaction $Cs^+ + F^- + Kr$ as well as the b_R (lines *3*) and b_i (lines *4*) opacity functions of the recombination reaction $Cs^+ + I^- + Kr$ at: (a) $E_i = E_R = 1$ eV, (b) $E_i = 1$ eV and $E_R = 5$ eV, (c) $E_i = 5$ eV and $E_R = 1$ eV, (d) $E_i = E_R = 5$ eV. All the opacity functions pertain to the case $T_{del} = 0$. The recombination probabilities are presented in units of 10^{-4}, i.e., the probability values are 10^4 times smaller than the numbers indicated on the ordinate axes.

and all the trends in the behavior of the opacity functions noted in the work [33] for R = Ar and Xe persist also for R = Kr. These trends consist in the following.

First, as a rule, the graphs of the b_i opacity functions of the reactions (6) are more symmetric with respect to the maximum position than the graphs of the b_R opacity functions, and the maximum of the b_R opacity function is higher than that of the b_i opacity function and is shifted "to the left", i.e., toward smaller values of the impact parameter (see Fig. 2). The exceptions to this rule are the opacity functions of the reaction $Cs^+ + F^- + Kr$ for the collision energies $(E_i, E_R) = (5, 1)$ and (5, 5) (in eV).

Second, for the reaction $Cs^+ + F^- + Kr$, as a rule, the value of $b_{R,lim}$ is considerably larger than the value of $b_{i,lim}$, while for the reaction $Cs^+ + I^- + Kr$, the opposite inequality is typical (see Table 3). Due to the presence of the Coulomb term $-1/r$, the potential (4) of the interaction between the ions is much longer-ranged than the potentials (5) of the interactions between the third body and each of the ions, so the inequality $b_{R,lim} > b_{i,lim}$ may seem paradoxical. However, as we noted in the work [33], while the impact

Table 3. The maximal values $b_{R,lim}$, $b_{i,lim}$ (rounded to the least exceeding integer in a.u.) of the impact parameters b_R, b_i for which we observed the recombination reactions (6) at $T_{del} = 0$

Collision energies (E_i, E_R), eV	(1, 1)	(1, 5)	(5, 1)	(5, 5)
Reaction $Cs^+ + F^- + Kr$	60; 34	27; 34	51; 29	59; 29
Reaction $Cs^+ + I^- + Kr$	15; 35	13; 35	47; 29	14; 31

The procedure of rounding a positive number to the least exceeding integer (also known as rounding up) consists in the following: the fraction part is removed and the integer obtained is increased by one (for instance, 28.137 is rounded to 29).

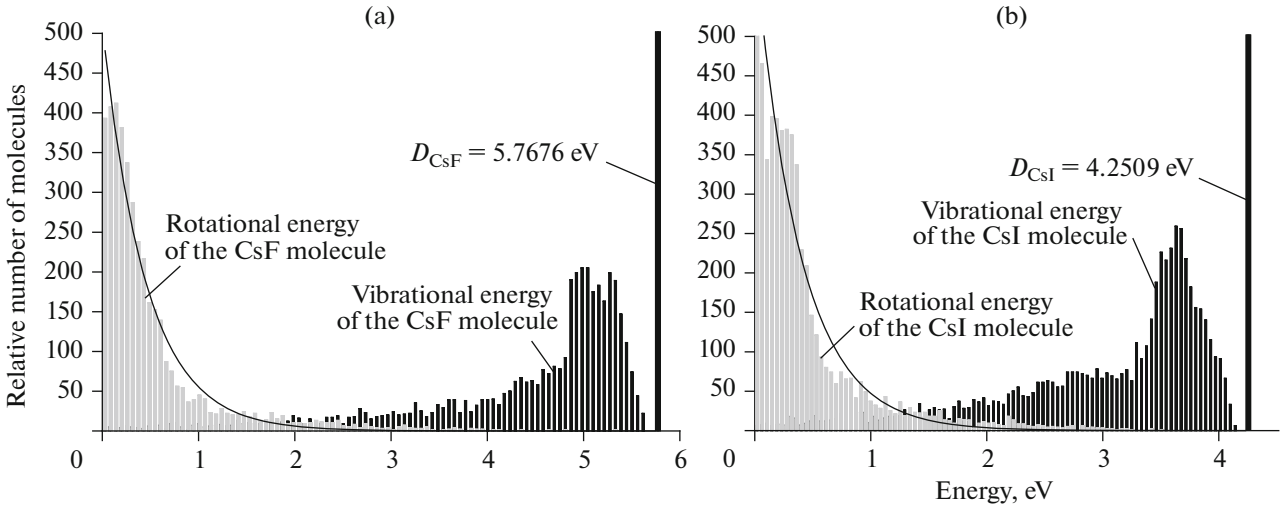

Fig. 3. The distributions of the vibrational (the black columns) and rotational (the grey columns) energies of: (a) the product CsF of recombination $Cs^+ + F^- + Kr$, (b) the product CsI of recombination $Cs^+ + I^- + Kr$ at $E_i = E_R = 1$ eV and $T_{del} = 0$. The solid lines show the Boltzmann rotational distributions at temperatures of: (a) 5885 K, (b) 5115 K. The potential well depths D of the ionic interaction potentials in the salt molecules CsF and CsI are also indicated.

parameter b_i of the ion encounter is related to the distance between the ions, the impact parameter b_R of the third body is related to the distance between the neutral atom R and the center of mass of the ion pair rather than to the distances between the R atom and the ions themselves. The internuclear distance between the R atom and one of the ions can be much smaller than the distance between the R atom and the center of mass of the ion pair. This phenomenon is more pronounced in the case where the center of mass of the ion pair is shifted to one of the ions (i.e., the masses of the ions are noticeably different) and the R atom approaches the ion pair from the side of the lighter ion from which the center of mass of the ion pair is far away. That is why the inequality $b_{R,lim} > b_{i,lim}$ is typical for the reactions (1) with $X^- = F^-$ and R = Ar, Kr, Xe but not for the reactions (1) with $X^- = I^-$. Besides that, one sees in Table 3 that the value of $b_{R,lim}$ varies over a far wider range than the value of $b_{i,lim}$.

In all our previous works where we considered statistical dynamics of direct three-body recombination reactions (1) for various halide ions X^- and neutral atoms R, the vibrational energy distributions of the salt molecules CsX turned out to be strongly non-equilibrium (as a rule, with a high population of vibrational levels with energies close to the bond energy), while the rotational energy distributions turned out to be almost equilibrium [19–22, 26, 27, 30–33]. This holds for calculations with both central ($b_i = 0$) and non-central encounters of the ions. The recombination reactions (6) with non-central encounters of the ions were no exception. To provide an example, in Fig. 3 we present the distributions of the vibrational and rotational energies of the products of the reactions (6) at $E_i = E_R = 1$ eV and $T_{del} = 0$.

At $T_{del} = 0$ and $(E_i, E_R) = (1, 1), (1, 5), (5, 1), (5, 5)$ (in eV), the temperatures T corresponding to the Boltzmann rotational distributions that best approximate the rotational energy distributions of the products of the reactions (6) are equal to 5885, 5004, 6202, 6579 K, respectively, for the reaction $Cs^+ + F^- + Kr$ and are equal to 5115, 4763, 6553, 5777 K, respectively, for the reaction $Cs^+ + I^- + Kr$. Thus, for the reaction $Cs^+ + F^- + Kr$, the temperatures T are arranged in the order $T_{5,5} > T_{5,1} > T_{1,1} > T_{1,5}$, while for the reaction $Cs^+ + I^- + Kr$, they are arranged in the order $T_{5,1} > T_{5,5} > T_{1,1} > T_{1,5}$ (the same order as for the reaction $Cs^+ + F^- + Xe$ [33]).

5. CONCLUSIONS

The results of the present paper show that the reactions of direct three-body recombination (6) exhibit almost all the main peculiarities of statistical dynamics of the reactions (1) with $X^- = F^-$, I^- found out in the work [33] for the case where the third body R is an argon or xenon atom. On the other hand, each of the six reactions (1) explored in the paper [33] and in the present work possesses its own dynamical characteristics, and many features of the dynamics of the reactions (1) with $X^- = F^-$, I^- and R = Kr cannot be predicted when one knows just the dynamics of the reactions (1) with $X^- = F^-$, I^- and R = Ar, Xe. Such dynamical properties of the reactions (1) include, for example, details of the structure of the excitation

function at $T_{del} = 0$, the general shape of the excitation function at $T_{del} = 0.2$ (at this value of T_{del}, the structures of the excitation functions of the four reactions (1) with $X^- = F^-$, I^- and R = Ar, Xe are very different [33]), details of the behavior of the opacity functions and of the distributions of the vibrational and rotational energies of the CsX products (in particular, the temperature T of the Boltzmann rotational distribution that best approximates the rotational energy distribution of the CsX molecules).

The complicated features of the dynamics of the direct three-body recombination reactions (1) necessitate studying detailed dynamics of these reactions. In the recent paper [34], we presented the results of visualization and a minute step-by-step analysis of nine trajectories which describe recombination (1) with $X^- = F^-$, I^- and R = Ar, Xe at $T_{del} = 0$, $E_R = 1$ eV, and $E_i = 1$ or 5 eV. These trajectories exhibit different mechanisms of energy transfer from the ion pair to the third body. In particular, energy transfer can occur via an encounter of the R atom with the Cs^+ ion, via an encounter of the R atom with the X^- ion, via successive encounters of the R atom with both the ions, and via an "insertion" of the R atom between the ions. At the same time, to explain the peculiarities of the structure of the excitation functions and of the opacity functions of the reactions (1) or those of the distributions of the vibrational and rotational energies of the products (and even to explain the fact that the vibrational energy distributions are strongly non-equilibrium whereas the rotational energy distributions are close to equilibrium ones), further research is needed.

FUNDING

This work was carried out within the framework of the theme "Physicochemical problems of energy industry and ecology" of the Program of fundamental scientific research of the state academies of sciences.

ADDITIONAL INFORMATION

The article was translated by the authors.

CONFLICT OF INTEREST

The authors declare that they have no conflicts of interest.

REFERENCES

1. D. L. Baulch, C. J. Cobos, R. A. Cox, et al., J. Phys. Chem. Ref. Data **21**, 411 (1992). https://doi.org/10.1063/1.555908
2. R. T. Pack, R. B. Walker, and B. K. Kendrick, J. Chem. Phys. **109**, 6701 (1998). https://doi.org/10.1063/1.477348
3. G. A. Parker, R. B. Walker, B. K. Kendrick, and R. T. Pack, J. Chem. Phys. **117**, 6083 (2002). https://doi.org/10.1063/1.1503313
4. O. P. Korobeinichev, A. G. Shmakov, V. M. Schwarzberg, T. A. Bolshova, D. A. Knyazkov, and S. A. Trubachev, Russ. J. Phys. Chem. B **15**, 433 (2021). https://doi.org/10.1134/S1990793121030076
5. G. Yin, J. Li, M. Zhou, et al., Combust. Flame **238**, 111915 (2022). https://doi.org/10.1016/j.combustflame.2021.111915
6. B. A. Knyazev, *Low Temperature Plasma and Gas Discharge* (Novosib. Gos. Univ., Novosibirsk, 2003) [in Russian].
7. V. E. Golant, A. P. Zhilinskii, and I. E. Sakharov, *Fundamentals of Plasma Physics* (Lan', St Petersburg, 2011; Wiley, New York, 1980).
8. V. N. Kondrat'ev and E. E. Nikitin, *Gas-Phase Reactions: Kinetics and Mechanisms* (Nauka, Moscow, 1974; Springer, Berlin, 1981).
9. I. A. Semiokhin, B. V. Strakhov, and A. I. Osipov, *Kinetics of Chemical Reactions* (Mosk. Gos. Univ., Moscow, 1995) [in Russian].
10. E. T. Denisov, O. M. Sarkisov, and G. I. Likhtenshtein, *Chemical Kinetics* (Khimiya, Moscow, 2000; Elsevier, Amsterdam, 2003).
11. A. L. Perkel' and S. G. Voronina, Russ. Chem. Bull. **69**, 2031 (2020). https://doi.org/10.1007/s11172-020-2999-9
12. A. M. Efremov, V. I. Svettsov, and V. V. Rybkin, *Vacuum-Plasma Processes and Technologies* (Ivanovo Gos. Univ. Khim. Tekhnol., Ivanovo, 2006) [in Russian].
13. G. V. Golubkov, V. L. Bychkov, V. O. Gotovtsev, S. O. Adamson, Yu. A. Dyakov, I. D. Rodionov, and M. G. Golubkov, Russ. J. Phys. Chem. B **14**, 351 (2020). https://doi.org/10.1134/S1990793120020219
14. G. V. Golubkov, T. A. Maslov, V. L. Bychkov, O. P. Borchevkina, S. O. Adamson, Yu. A. Dyakov, A. A. Lushnikov, and M. G. Golubkov, Russ. J. Phys. Chem. B **14**, 853 (2020). https://doi.org/10.1134/S199079312005019X
15. A. Roth, B. Drummond, E. Hébrard, et al., Mon. Not. R. Astron. Soc. **505**, 4515 (2021). https://doi.org/10.1093/mnras/stab1256
16. A. V. Eletskii, Sov. Phys. Usp. **21**, 502 (1978). https://doi.org/10.1070/PU1978v021n06ABEH005558
17. V. F. Tarasenko and S. I. Yakovlenko, Quantum Electron. **27**, 1111 (1997). https://doi.org/10.1070/QE1997v027n12ABEH001103
18. A. M. Boichenko, V. F. Tarasenko, and S. I. Yakovlenko, Laser Phys. **10**, 1159 (2000).
19. V. M. Azriel', D. B. Kabanov, L. I. Kolesnikova, and L. Yu. Rusin, Izv. Akad. Nauk, Energet., No. 5, 50 (2007).
20. V. M. Azriel' and L. Yu. Rusin, Russ. J. Phys. Chem. B **2**, 499 (2008). https://doi.org/10.1134/S1990793108040015
21. V. M. Azriel', Doctoral (Phys. Math.) Dissertation (Inst. Energy Probl. Chem. Phys. RAS, Moscow, 2008).

22. V. M. Azriel', E. V. Kolesnikova, L. Yu. Rusin, and M. B. Sevryuk, J. Phys. Chem. A **115**, 7055 (2011). https://doi.org/10.1021/jp112344j
23. D. B. Kabanov and L. Yu. Rusin, Chem. Phys. **392**, 149 (2012). https://doi.org/10.1016/j.chemphys.2011.11.009
24. D. B. Kabanov and L. Yu. Rusin, Russ. J. Phys. Chem. B **6**, 475 (2012). https://doi.org/10.1134/S1990793112040033
25. E. V. Kolesnikova and L. Yu. Rusin, Russ. J. Phys. Chem. B **6**, 583 (2012). https://doi.org/10.1134/S1990793112050156
26. V. M. Azriel', L. Yu. Rusin, and M. B. Sevryuk, Chem. Phys. **411**, 26 (2013). https://doi.org/10.1016/j.chemphys.2012.11.016
27. E. V. Ermolova, Candidate (Phys. Math.) Dissertation (Tal'rose Inst. Energy Probl. Chem. Phys. RAS, Moscow, 2013).
28. E. V. Ermolova and L. Yu. Rusin, Russ. J. Phys. Chem. B **8**, 261 (2014). https://doi.org/10.1134/S199079311403004X
29. E. V. Ermolova, L. Yu. Rusin, and M. B. Sevryuk, Russ. J. Phys. Chem. B **8**, 769 (2014). https://doi.org/10.1134/S1990793114110037
30. V. M. Azriel', L. I. Kolesnikova, and L. Yu. Rusin, Russ. J. Phys. Chem. B **10**, 553 (2016). https://doi.org/10.1134/S1990793116040205
31. V. M. Azriel', V. M. Akimov, E. V. Ermolova, et al., Prikl. Fiz. Mat., No. 2, 30 (2018).
32. V. M. Azriel', V. M. Akimov, E. V. Ermolova, D. B. Kabanov, L. I. Kolesnikova, L. Yu. Rusin, and M. B. Sevryuk, Russ. J. Phys. Chem. B **12**, 957 (2018). https://doi.org/10.1134/S1990793118060131
33. V. M. Akimov, V. M. Azriel', E. V. Ermolova, et al., Phys. Chem. Chem. Phys. **23**, 7783 (2021). https://doi.org/10.1039/d0cp04183a
34. V. M. Akimov, V. M. Azriel', E. V. Ermolova, et al., Phys. Chem. Chem. Phys. **24**, 3129 (2022). https://doi.org/10.1039/d1cp04362e
35. V. M. Azriel', V. M. Akimov, E. V. Ermolova, D. B. Kabanov, L. I. Kolesnikova, L. Yu. Rusin, and M. B. Sevryuk, Russ. J. Phys. Chem. B **15**, 935 (2021). https://doi.org/10.1134/S1990793121060142
36. E. K. Parks, M. Inoue, and S. Wexler, J. Chem. Phys. **76**, 1357 (1982). https://doi.org/10.1063/1.443129
37. E. K. Parks, L. G. Pobo, and S. Wexler, J. Chem. Phys. **80**, 5003 (1984). https://doi.org/10.1063/1.446523
38. F. P. Tully, N. H. Cheung, H. Haberland, and Y. T. Lee, J. Chem. Phys. **73**, 4460 (1980). https://doi.org/10.1063/1.440683
39. V. M. Azriel', D. B. Kabanov, and L. Yu. Rusin, Russ. J. Phys. Chem. B **5**, 177 (2011). https://doi.org/10.1134/S1990793111020175
40. P. Brumer and M. Karplus, J. Chem. Phys. **58**, 3903 (1973). https://doi.org/10.1063/1.1679747
41. P. Brumer, Phys. Rev. A **10**, 1 (1974). https://doi.org/10.1103/PhysRevA.10.1
42. S. H. Patil, J. Chem. Phys. **86**, 7000 (1987). https://doi.org/10.1063/1.452348
43. S. H. Patil, J. Chem. Phys. **89**, 6357 (1988). https://doi.org/10.1063/1.455403
44. A. D. Koutselos, E. A. Mason, and L. A. Viehland, J. Chem. Phys. **93**, 7125 (1990). https://doi.org/10.1063/1.459436
45. T. L. Gilbert, O. C. Simpson, and M. A. Williamson, J. Chem. Phys. **63**, 4061 (1975). https://doi.org/10.1063/1.431848
46. I. R. Gatland, M. G. Thackston, W. M. Pope, et al., J. Chem. Phys. **68**, 2775 (1978). https://doi.org/10.1063/1.436069
47. H. Inouye, K. Noda, and S. Kita, J. Chem. Phys. **71**, 2135 (1979). https://doi.org/10.1063/1.438586
48. L. A. Viehland, Chem. Phys. **85**, 291 (1984). https://doi.org/10.1016/0301-0104(84)85040-5
49. C. C. Kirkpatrick and L. A. Viehland, Chem. Phys. **98**, 221 (1985). https://doi.org/10.1016/0301-0104(85)80135-X
50. L. Yu. Rusin and M. B. Sevryuk, TsITiS Report No. AAAA-B16-216092340017-7 (Tal'rose Inst. Energy Probl. Chem. Phys. RAS, Moscow, 2016).
51. Yu. N. Blagoveshchenskii, *Secrets of Correlations in Statistics* (Nauchnaya Kniga, INFRA-M, Moscow, 2009) [in Russian].
52. M. B. Lagutin, *Visual Mathematical Statistics* (BINOM, Labor. Znanii, Moscow, 2011) [in Russian].